Supplementary information for

Facile functionalization of polypeptide by thiol-yne photochemistry for biomimetic materials synthesis

Yugang Huang,[a] Yonghong Zeng,[a] Jianwen Yang,*[a,b] Zhaohua Zeng,[a,b] Fangming Zhu,*[a,b] and Xudong Chen[a,b]

[a] *Designed Synthesis and Application of Polymer Material Lab, Institute of Polymer Science, School of Chemistry and Chemical Engineering, Sun Yat-Sen University, Guangzhou 510275, China.Tel: +86-20-8411-1138; Email:cesyjw@mail.sysu.edu.cn.*
[b] *Key Laboratory for Polymer Composite and Functional Materials of Ministry of Education, School of Chemistry and Chemical Engineering, Sun Yat-Sen University, GuangZhou, China. Email: ceszfm@mail.sysu.edu.cn.*

Content

1 Materials

L-glutamic acid (99%, +30.5º~32.5º), propargyl alcohol (99%) and triphosgene (99%) were purchased from Aladdin-reagent (China) and used as received. Amine-terminated poly(ethylene glycol) (PEO-NH_2, *M*n= 5000 g mol^{-1}), poly (propylene oxide) bis (2-aminopropyl ether) (NH_2-PPO-NH_2, *M*n= 4000 g mol^{-1}), thioglycolic acid (99%), mercaptopropionic acid (97%) and 1-thioglycerol (95%) were purchased from Sigma-Aldrich and used as received. Dichloromethane (CH_2Cl_2) was dried over calcium chloride, refluxed with calcium hydride (CaH_2) and then distilled. *N,N*-dimethyl formaminde (DMF) was dried over CaH_2 and then distilled under vacuum. Tetrahydrofuran was refluxed with lithium aluminium hydride ($LiAlH_4$) and then distilled. A medium pressure mercury lamp (λ_{max} = 365 nm, 20 mW cm^{-2}) was used for thiol-yne photochemistry.

2 Methods

^{1}H NMR spectra were recorded at room temperature on a Varian 300 MHz spectrometer and unless otherwise stated deuterated methyl sulfoxide (DMSO-d_6) was used as solvent; Size exclusion chromatography (SEC) was performed on a Waters system in DMF with 0.01 mol L^{-1} LiBr at 50 ℃ against polystyrene standards, operating at 1.0 mL min^{-1}; Fourier transform infrared (FTIR) spectra were recorded on a Thermo Nicolet/Nexus 670 spectrophotometer and unless otherwise stated the attenuated total reflection (ATR) method is used; Circular dichroism (CD) spectra were performed on a JASCO J-810 spectrometer at room temperature using water as solvent. The target polymers were first dissolved in 0.1 M NaOH with a concentration of 4 mg mL^{-1}. The samples were obtained by diluting the mother solution, and then 0.1 M HCl was used to adjust the pH to desired value; Tapping mode AFM in air was performed on a SHIMADZU 9500J3 SPM. Samples were prepared according to the methods described in CD measurements. A drop of solution was deposited on freshly cleaved mica surface and the water was removed by evaporation at room temperature in a desiccator; Transmission electron microscopy (TEM) observation was performed on a JEM-2010HR system. A drop of the sample solution mentioned above was deposited on carbon coated copper grids for 1 minute and followed by staining with 0.5 wt % aqueous solution of phosphotungstic acid; JSM-6330F scanning electron microscopy (SEM) was used for the morphology observation of $CaCO_3$. 1FP was first dissolved in 0.1 M NaOH, and then the pH value of the solution was adjusted with 1 M HCl. Finally 1FP solution with concentration of 1 mg mL^{-1} and pH value of 10 or 12 was obtained. Then 0.16 mL of an aqueous 0.5 M $CaCl_2$ solution and 0.16 mL of an aqueous 0.5 M Na_2CO_3 were added into 5 mL of 1FP aqueous solution with a speed of 0.03 mL min^{-1}. After 7 days, a drop of the solution was deposited on glass slide for 10 minutes, and then the water was removed with a piece of filter paper.

3 Dynamic Light Scattering (DLS) and static Light Scattering (SLS)measurements

Variable-angle DLS measurement was made using incident light at 532 nm. The angular dependence of the autocorrelation functions was measured using a Brookhaven Instruments BI-200SM goniometer. Apparent diffusion coefficients (D_{app}) were calculated based on the Equation (1):

$$\Gamma = D_{app} q^2 \quad (1)$$

where,

Γ— the decay rate;

q— scattering vector.

q is given by Equation (2):

$$q = \frac{4\pi n}{\lambda}\sin\frac{\theta}{2} \tag{2}$$

where,

q— scattering vector;

λ— the wavelength of the incident laser;

θ— the scattering angle;

n— the refractive index of the media.

The hydrodynamic radius (R_h) was then calculated from the Stokes–Einstein Equation (3):

$$R_h = \frac{k_B T}{6\pi\eta D_{app}} \tag{3}$$

where,

k_B —Boltzmann constant;

T —temperature;

η —the viscosity of the medium;

D_{app} —apparent diffusion coefficient.

Angular–dependent static light scattering (SLS) experiments were performed with the same instrument mentioned above. The radius of gyration (R_g) of the assemblies was determined from the angular dependence of the scattering intensity. A Zimm plot was used to determine the radius of gyration (Fig. S15).

Mother solution was prepared by dissolving $2FP_{33}$ into 0.1M NaOH aqueous solution with concentration of 4 mg mL^{-1}. Sample solutions were prepared by diluting the mother solution to different concentrations, adjusting the pH to desired values and sonicating for about an hour. Samples were filtered through a 0.45 μm filter directly into the scattering cell.

4 Experimental section

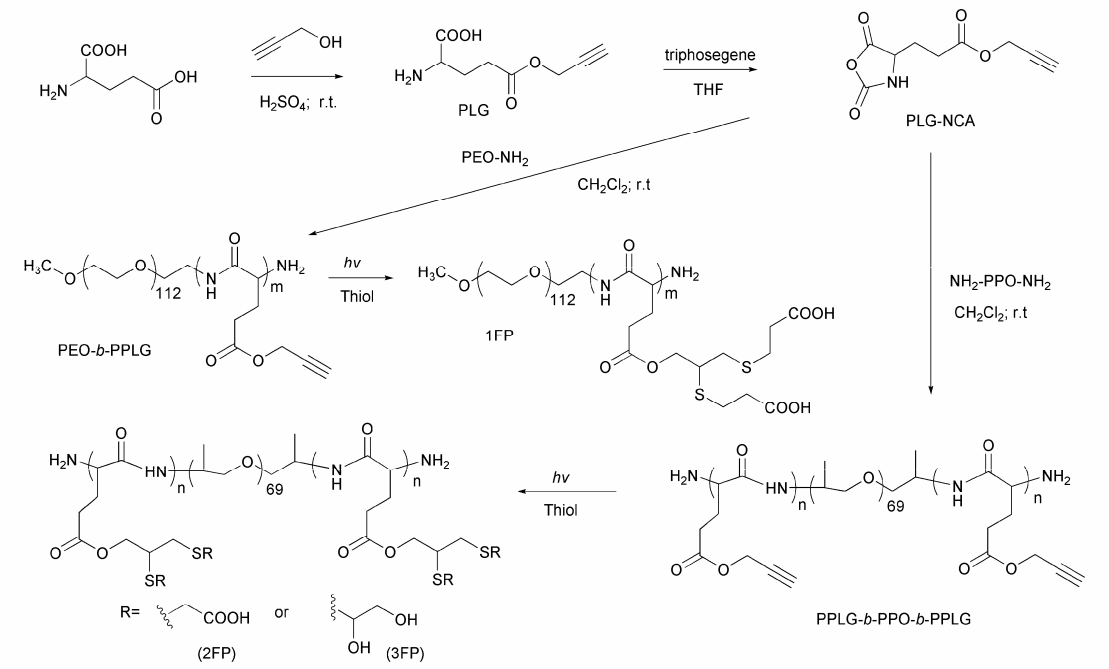

Scheme. S1 The synthetic route to prepare 1FP, 2FP and 3FP by combination of the ROP of PLG-NCA and thiol-yne click chemistry.

The synthetic route to prepare 1FP, 2FP and 3FP was depicted in Scheme S1.

4.1 Synthesis of γ-propargyl-L-glutamate (PLG) and γ-propargyl-L-glutamate N-carboxyanhydride (PLG-NCA)

L-glutamic acid (20 g, 0.14 mol) was suspended in propargyl alcohol (30 mL) at 0 °C. Then sulfuric acid (8 mL, 98%) was added dropwise over 30 min. After stirring at room temperature overnight, the mixture was heated to 55-60 °C, and the reaction was kept at this temperature for 4 hours. Then the viscous solution was cooled to RT and slowly poured into a mixture of sodium bicarbonate ($NaHCO_3$) (27 g) and water (200 mL). Then additional $NaHCO_3$ was carefully added to keep the pH at 7.0. The obtained mixture was then concentrated to 120-150 mL and placed at 4 °C overnight. The crude precipitate was filtered and washed with enough methanol. Finally 11.68 g dry PLG was obtained. Yield: 46 %.

PLG (4.1 g, 0.022 mol) was suspended in anhydrous THF (100 mL) in a reaction flask fitted with a reflux condenser and N_2 bubbler. After heating to 50 °C, triphosgene (2.2 g, 7.33×10^{-3} mol) was added and the reaction solution became clear at once. After 30 minutes the reaction solution was cooled to RT and then poured into *n*-hexane (300 mL). The mixture was placed at -20 °C overnight, and then a slightly brown liquid appeared at the bottom of the flask. After removing the supernatant, the brown oil was collected and redissolved in 100 mL of ethyl acetate, followed by washing with 100 mL ice-cold water and 50 mL of 0.5 % $NaHCO_3$ ice-cold aqueous solution. The organic phase was then dried over anhydrous $MgSO_4$ and evaporated to give 1.8 g of PLG-NCA as a viscous liquid. Yield: 38 %. The methods for the synthesis and purification of PLG-NCA are proposed according to the previous work.[S1]

^{1}H NMR of PLG, δ_H (300 MHZ, D_2O): 2.10 (dm, 2H, CH2CH_2-CO), 2.49 (t, 2H,CH_2CH_2-CO), 2.80 (t, 1H, C≡CH), 3.65 (t,1H, -CH-CH_2CH_2CO), 4.63 (d, 2H, COO CH_2-C≡CH).

^{1}H NMR of PLG-NCA, δ_H (300 MHz, $CDCl_3$): 2.18 (dm, 2H, CH2CH_2-CO), 2.52 (t, 1H, C≡CH), 2.60 (t, 2H,CH_2CH_2-CO), 4.44 (t,1H, -CH-CH_2CH_2COO), 4.69 (d, 2H, COOCH_2-C≡CH), 6.98 (s, br, 1H, -CONH-).

4.2 Synthesis of PEO-b-PPLG and PPLG-b-PPO-b-PPLG

The methods for synthesis of PEO-*b*-PPLG and PPLG-*b*-PPO-*b*-PPLG are similar, and thus here a typical synthesis of PEO-*b*-PPLG was described as follows: PLG-NCA (0.8 g, 3.70×10^{-3} mol) was introduced into a Schlenk flask and dissolved with anhydrous CH_2Cl_2 (12 mL), and the solution was then bubbled with N_2 for 20 minutes. At this time 8 mL CH_2Cl_2 solution containing PEO-NH_2 (0.12 g, 2.47×10^{-5} mol) was added *via* a syringe. Additional 10 minutes of bubbling with N_2 was taken to degas the solution, and then the flask was sealed. After stirring at room temperature for 3 days, 0.65 g of copolymer was recovered by precipitation in diethyl ether and dried under vacuum. Yield: 87 % (by gravimetric analysis).

4.3 Functionalization of PEO-b-PPLG and PPLG-b-PPO-b-PPLG by thiol-yne photochemistry

As an example, the synthesis of 1FP was described as follows: PEO-*b*-PPLG (0.1 g, 5.04×10^{-4} mol of alkynes) was dissolved with DMF (2.5 mL). Then mercaptopropionic acid (MPA) (0.22 g, 2.02×10^{-3} mol of thiols) and UV 651 (11.6 mg) were introduced into the flask. The reaction solution was stirred at room temperature and irradiated with a medium pressure mercury light (365 nm, 20 mW cm^{-2}) for 60 minutes . The resulting solution was diluted with DMF and then purified by dialysis against methanol to remove unreacted thiols. Yield is quantitative (by gravimetric analysis).

5 Characterization of all the obtained polypeptide-based hybrid copolymers

5.1 Characterization of ^{1}H NMR

5.1.1 ^{1}H NMR of PEO-b-PPLG and 1FP

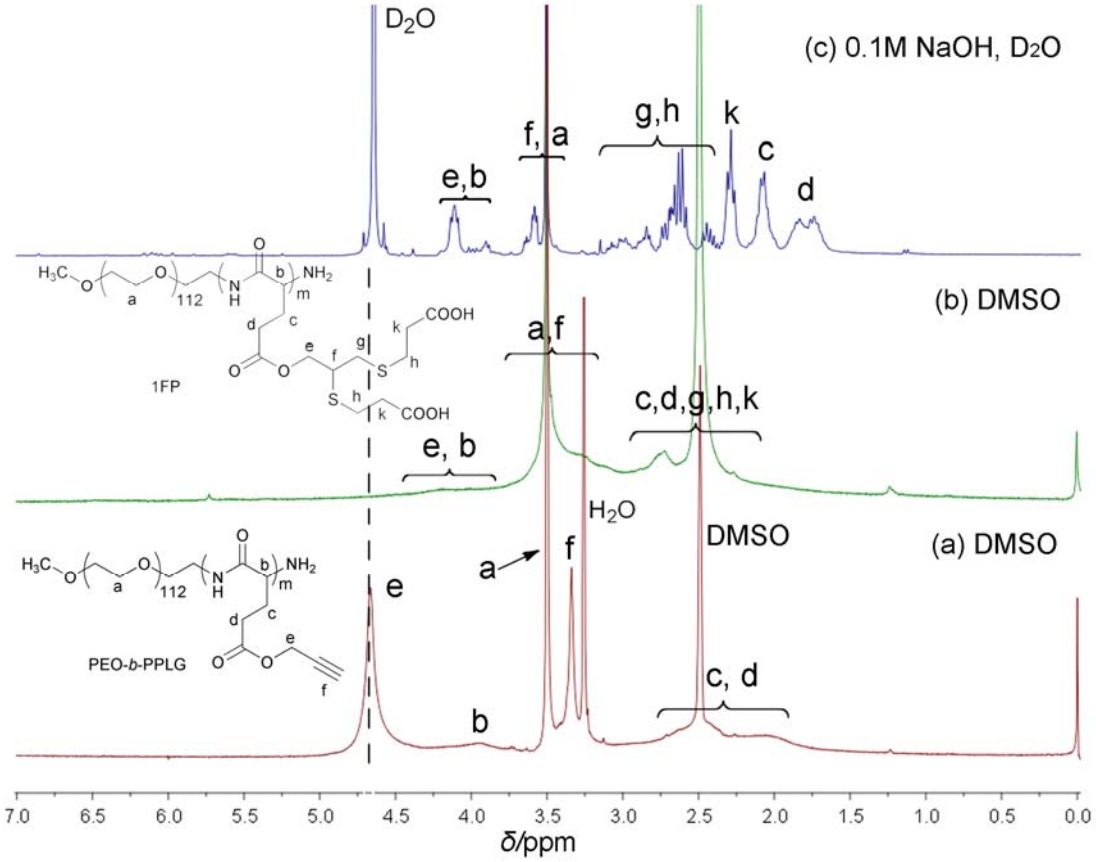

Fig. S1 ^{1}H NMR spectra of PEO-*b*-PPLG and 1FP in d_6-DMSO (a,b) or 0.1 M NaOH deuterium oxide solution (c).

The ^{1}H NMR spectra of PEO-*b*-PPLG and 1FP with peak assignments were shown in Fig. S1. It clearly shows that the peak of methylene groups adjacent to alkyne at 4.7 ppm completely disappeared after 60 minutes of the thiol-yne click reaction. In Fig. S1 (b), overlap of the peaks is caused by the limited solubility of 1FP resulting from the introduction of abundant carboxyl acid groups. A clear assignment of the peaks is available by dissolving 1FP in 0.1 M NaOH deuterium oxide solution (Fig. S1 (c)).

It should be noted that the DP mentioned above only means the number-average degree of polymerization of the polypeptide segments. Because the number of the repeated units of PEO blocks (112) has been known, DP of PPLG blocks can be calculated based on the peak area of methylene groups adjacent to alkyne at 4.7 ppm. (peak e in Fig. S1) and the peak area of methenes (peak a in Fig. S1) of PEO blocks.

Assuming the number of polypeptide segments is N_1, and then it can be determined by ^{1}H NMR using the following Equation (4):

$$N_1 = \frac{448A_a}{2A_e} \quad (4)$$

where,

N_1 —*DP* of PEO-*b*-PPLG;

A_a —the area of peak *a* in Fig. S1 (a);

A_e —the area of peak e in Fig. S1 (a).

Thus, molecular weight of PEO-*b*-PPLG can be obtained according to the ^{1}H NMR, which is presented in Formula (1a), where the PEO has a molecular weight of 5000 g mol^{-1}, and per repeated unit of polypeptide has a molecular weight of 167 g mol^{-1}.

$$5000 + \frac{224A_a}{A_e} \times 167 \quad (1a)$$

5.1.2 ^{1}H NMR of PPLG-b-PPO-b-PPLG and 2FP

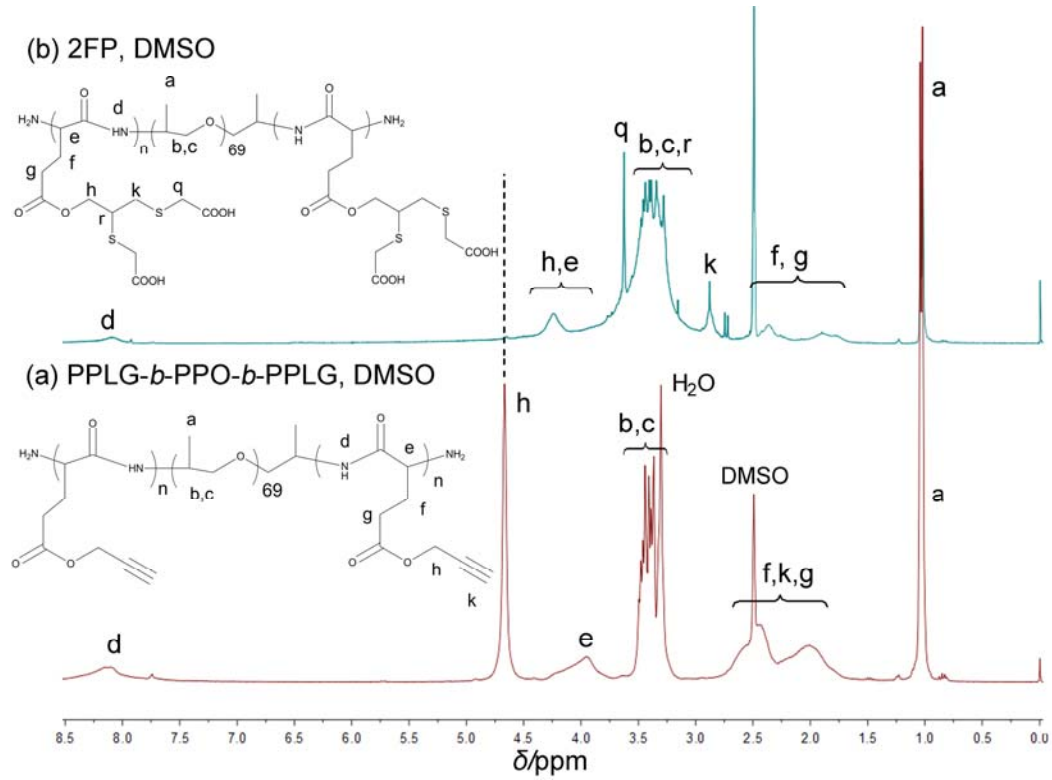

Fig. S2 ^{1}H NMR spectra of PPLG-*b*-PPO-*b*-PPLG (a) and 2FP (b) in d_6-DMSO.

The ^{1}H NMR spectra of PPLG-*b*-PPO-*b*-PPLG and 2FP with peak assignments were shown in Fig. S2. It clearly shows that the peak of methylene groups adjacent to alkyne at 4.7 ppm completely disappeared after 45 minutes of the thiol-yne click reaction between PPLG-PPO-PPLG and thioglycolic acid (TGA). Because the number of the repeated units of PPO blocks (70) has been known, *DP* of PPLG- PPO -PPLG can be calculated based on the peak area of methyl (peak *a* in Fig. S2) of PPO blocks and the peak area of methenes (peak *h* in Fig. S2) adjacent to alkynes. Thus, *DP* of PPLG-*b*-PPO-*b*-PPLG is given by Equation (5):

$$D_2 = \frac{3 \times 70A_h}{2A_a} \quad (5)$$

where,

D_2—*DP* of PPLG-*b*-PPO-*b*-PPLG ;

A_a —the area of peak *a* in Fig S2. (a);

A_h —the area of peak *h* in Fig S2. (a).

Further, molecular weight of PPLG-*b*-PPO-*b*-PPLG also can be obtained according to the ^{1}H NMR, which is presented in Formula (2a), where the PPO has a molecular weight of 4000 g mol^{-1}, and per repeated unit of polypeptide has a molecular weight of 167 g mol^{-1}.

$$4000 + \frac{3 \times 70A_h}{2A_a} \times 167 \quad (2a)$$

5.1.3 ^{1}H NMR of 3FP

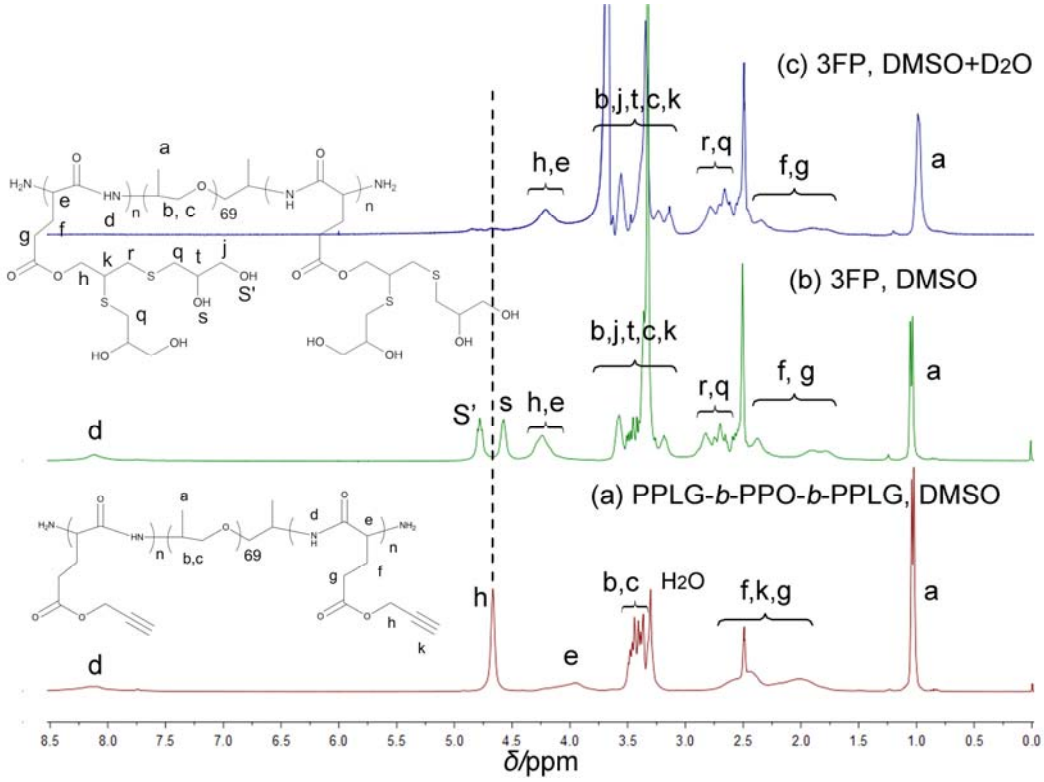

Fig. S3 ^{1}H NMR spectra of PPLG-*b*-PPO-*b*-PPLG in d_6-DMSO (a), 3FP in d_6-DMSO (b) or in d_6-DMSO + D_2O (one drop) (c).

The ^{1}H NMR spectra of PPLG-*b*-PPO-*b*-PPLG and 3FP with peak assignments were shown in Fig. S3. It clearly shows that the peak of methylene groups adjacent to alkyne at 4.7 ppm nearly disappeared after thiol-yne click reaction between PPLG-*b*-PPO-*b*-PPLG and 1-thioglycero (TGO) for 45 minutes. Two new peaks of hydroxyl group at 4.6 ppm and 4.8 ppm (S and S' in Fig. 3b) appeared. The two peaks disappeared while one drop of D_2O was added. Because these two peaks did not overlap with other peaks, grafting efficiency of PPLG-PPO-PPLG by TGO and molecular weight of 3FP can be calculated based on the number of the repeated units of PPO blocks. Thus, grafting efficiency (G_E) of PPLG-*b*-PPO-*b*-PPLG is given by Equation (6):

$$G_E = \frac{A_a}{4A_{a'}A_h}(A_s + A_{s'}) \times 100\% \qquad (6)$$

where,

G_E—grafting efficiency of PPLG-*b*-PPO-*b*-PPLG ;

A_a —the area of peak *a* in Fig S3. (a);

$A_{a'}$ —the area of peak *a* in Fig S3. (b);

A_s —the area of peak *s* in Fig S3. (b);

$A_{s'}$ —the area of peak *s'* in Fig S3. (b);

Further, molecular weight of 3FP also can be obtained according to the molecular weight of PPLG-*b*-PPO-*b*-PPLG (given by Formula (2a) and the grafting efficiency (G_E)), which is presented in Formula (3a):

$$D_2 \times 167 + 4000 + 2 \times 107 \times D_2 \times G_E \qquad (3a)$$

D_2—given by Formula (2a);

G_E—given by Equation (6).

where, PPO has a molecular weight of 4000 g mol^{-1}; per repeated unit of polypeptide has a

molecular weight of 167 g mol^{-1}; 1-thioglycero (TGO) has a molecular weight of 107 g mol^{-1}.

5.2 Characterization of size exclusion chromatography (SEC)

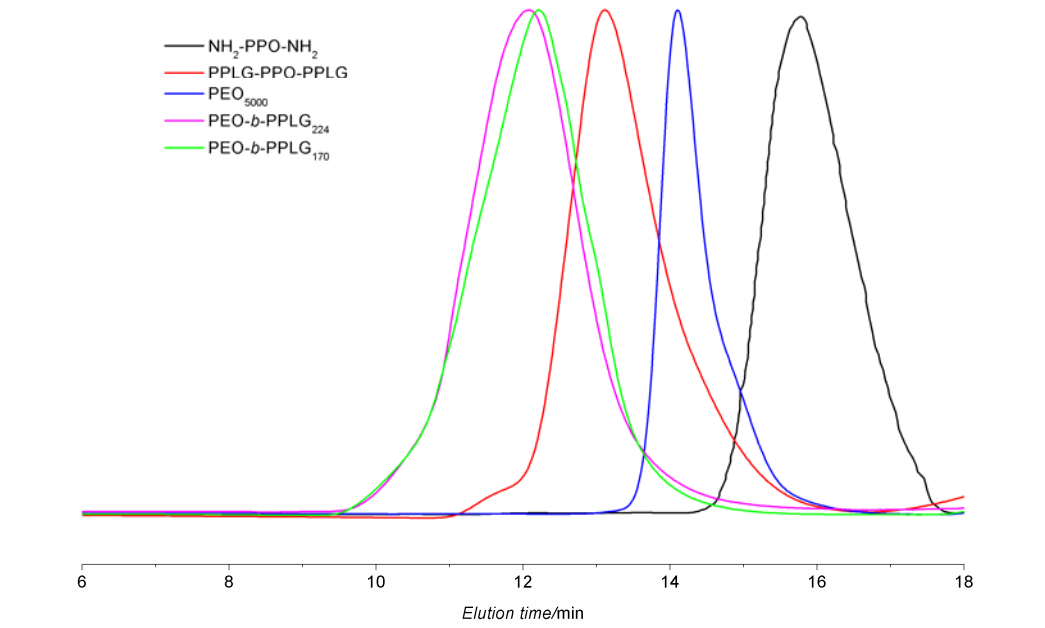

Fig. S4 Size exclusion chromatography curves of PEO-*b*-PPLG and PPLG-PPO-PPLG.

Fig. S4 shows the SEC curves of the obtained polypeptide hybrid copolymers. All products exhibit single peak and PDI of *ca.* 1.40, a common polydispersity of ROP of NCAs. However, the determination of molecular weight of 1FP, 2FP and 3FP had not been carried out by SEC because they have a poor solubility in most common solvents caused by the rigid polypeptide backbone and the introduced abundant functional groups at the side chains (-COOH and -OH). Nevertheless, their molecular weights were calculated based on the yields. Molecular weight of 3FP can be obtained by ^{1}H NMR, which is described in section of 5.1.3.

In summary, the molecular weights of all the hybrid copolymers were list in Table S1 by the combination of ^{1}H NMR, SEC and yield.

Table S1 Characteristics of all the obtained hybrid copolymers.

Polymer	[a] Mn/ g mol^{-1} ($\times 10^4$)	Mn/ g mol^{-1} ($\times 10^4$)	[e] DP	[a] PDI
PEO-*b*-PPLG$_{170}$	4.15	[b] 3.34	170	1.44
PEO-*b*-PPLG$_{224}$	4.27	[b] 4.24	224	1.37
PPLG$_{33}$-*b*-PPO-*b*-PPLG$_{33}$	2.50	[b] 1.50	66	1.42
1FP$_{170}$	-	[c] 7.62	170	-
1FP$_{224}$	-	[d] 8.78	224	-
2FP$_{33}$	-	[d] 3.56	66	-
3FP$_{33}$	-	[c] 3.75	66	-

[a] Determined by SEC in DMF at 50 ℃, 0.01 M LiBr. [b] Determined by ^{1}H NMR in d_6-DMSO. [c] Determined by by ^{1}H NMR in d_6-DMSO based on the conversion of alkynes (or grafting ratio of thiols). [d] Determined by yield of 1FP$_{224}$ and 2FP$_{33}$, respectively. [e] The polymerization degree of polypeptide blocks.

6 *Conversion of alkyne determined by ^{1}H NMR*

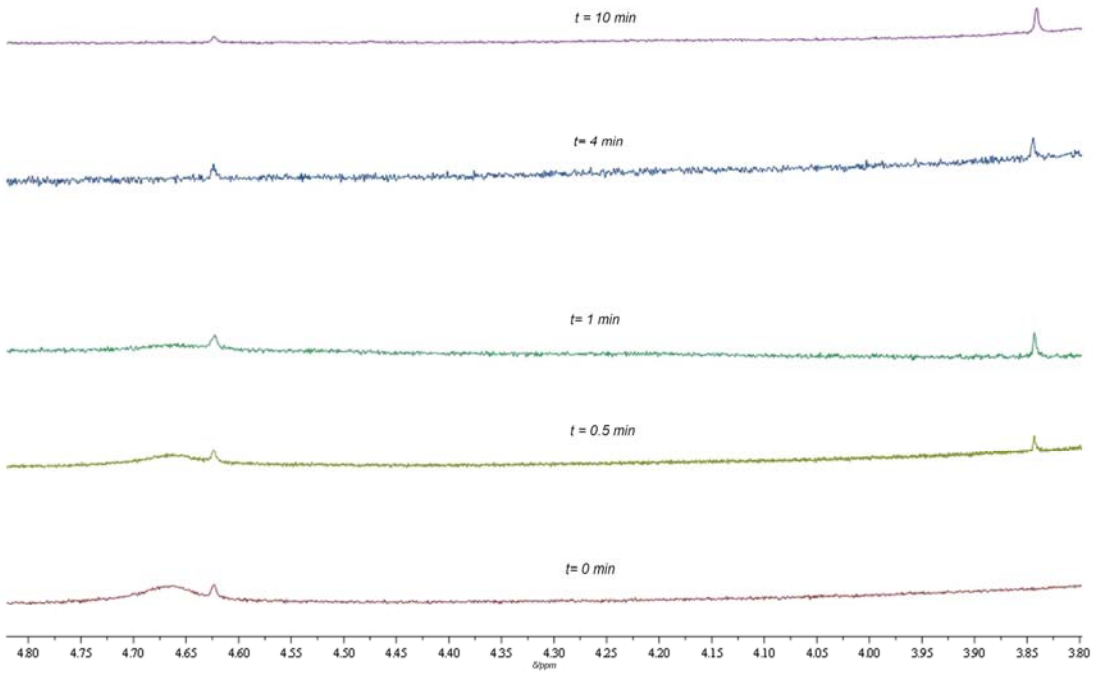

Fig. S5 Evolution of the ^{1}H NMR spectra for the photoreaction between PEO-*b*-PPLG$_{170}$ and MPA over irradiation time.

Conversion also can be determined from the ^{1}H NMR by recording the disappearance of the peak of methylene groups adjacent to alkyne at 4.7 ppm. In the unfunctionalized polymer we observed the methylene groups peak due to the propargyl ester linkage at 4.6-4.75 ppm, and upon irradiation these peaks appeared at 3.83 ppm in the reaction solution. A magnified region between 3.8-4.8 ppm was displayed in Fig. S5 with the purpose of the discrimination of the peak positions. The measurements were also carried out by sampling the reaction solutions at different irradiation time. Thus, conversion of alkyne can be calculated according to the Equation (7):

$$C = \frac{I_{3.83}}{I_{4.66} + I_{3.83}} \times 100\% \quad (7)$$

7 Secondary structure of the obtained polypeptide-based hybrid copolymers in bulk and water

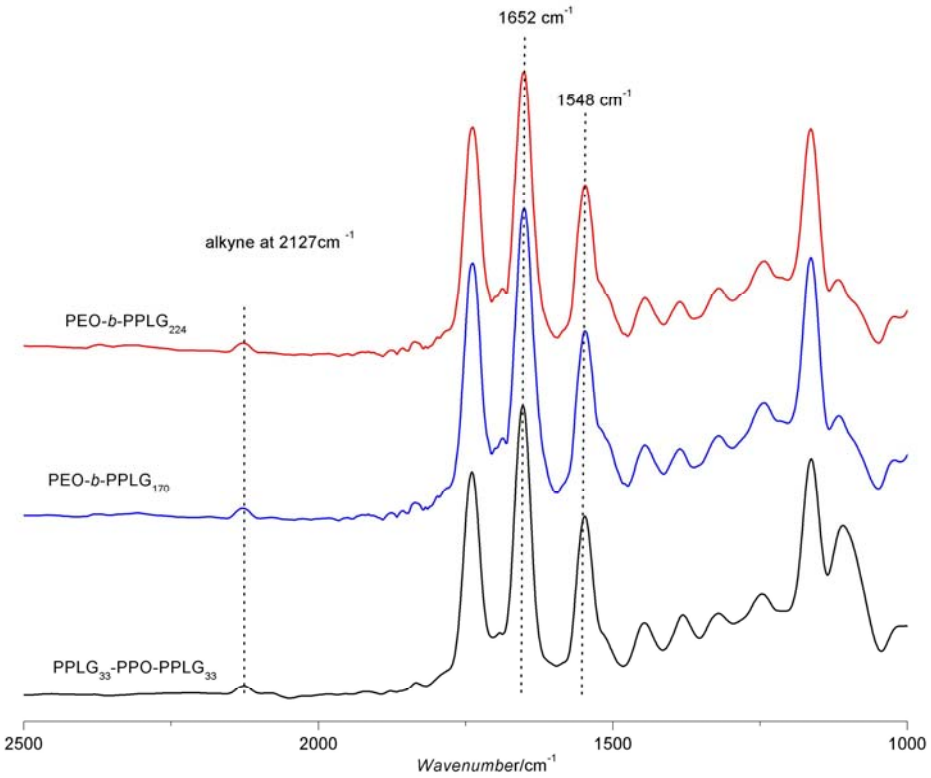

Fig. S6 ATR-FTIR spectra of PEO-*b*-PPLG$_{170,}$ PEO-*b*-PPLG$_{224}$ and PPLG$_{33}$-*b*-PPO-*b*-PPLG$_{33}$ between 1000-2500 cm^{-1}.

To present, researchers know little about the structural parameters and secondary structure of PPLG because it is a rather new clickable polypeptide. Hence, herein FTIR and Circular Dichroism spectroscopy (CD) are employed to investigate the secondary structure of PPLG blocks in bulk and water. FTIR are widely used to explore the secondary structure of polypeptides (e.g. Poly(γ-benzyl-L-glutamate).[3] Absorption of stretching of the C=O (amide I) at 1652 cm^{-1} and the deformation and stretching of the N-H bond (amide II) at 1548 cm^{-1} indicate the α-helix conformation adopted by the polypeptide.[2] Here all the hybrid polymers in bulk exhibit absorption band at 1652 and 1548 cm^{-1}, which is consistent with right-handed α-helix conformation. Typically, The ATR-FTIR spectra of PEO-*b*-PPLG$_{170,}$ PEO-*b*-PPLG$_{224}$ and PPLG-*b*-PPO-*b*-PPLG between 1000-2500 cm^{-1} were shown in Fig. S6.

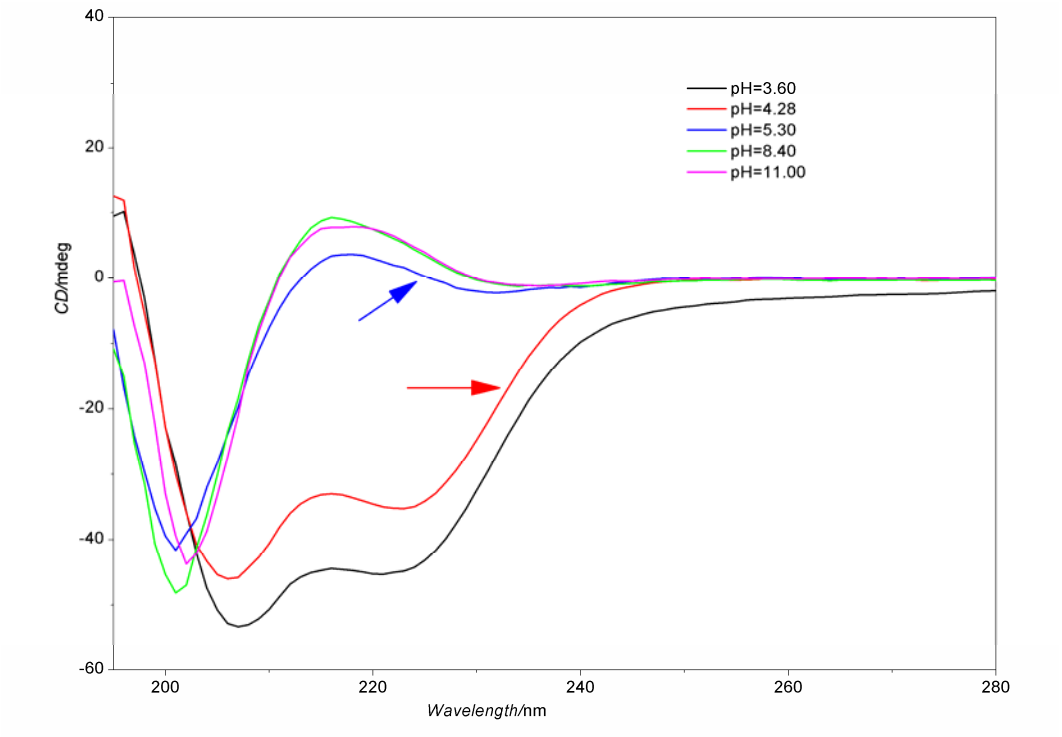

Fig. S7 CD spectra of $2FP_{33}$ in water at different pH values, 25 ℃, 0.2 mg mL^{-1}. Arrows indicate the transition region of random coil to α-helix comformation of polypeptide blocks.

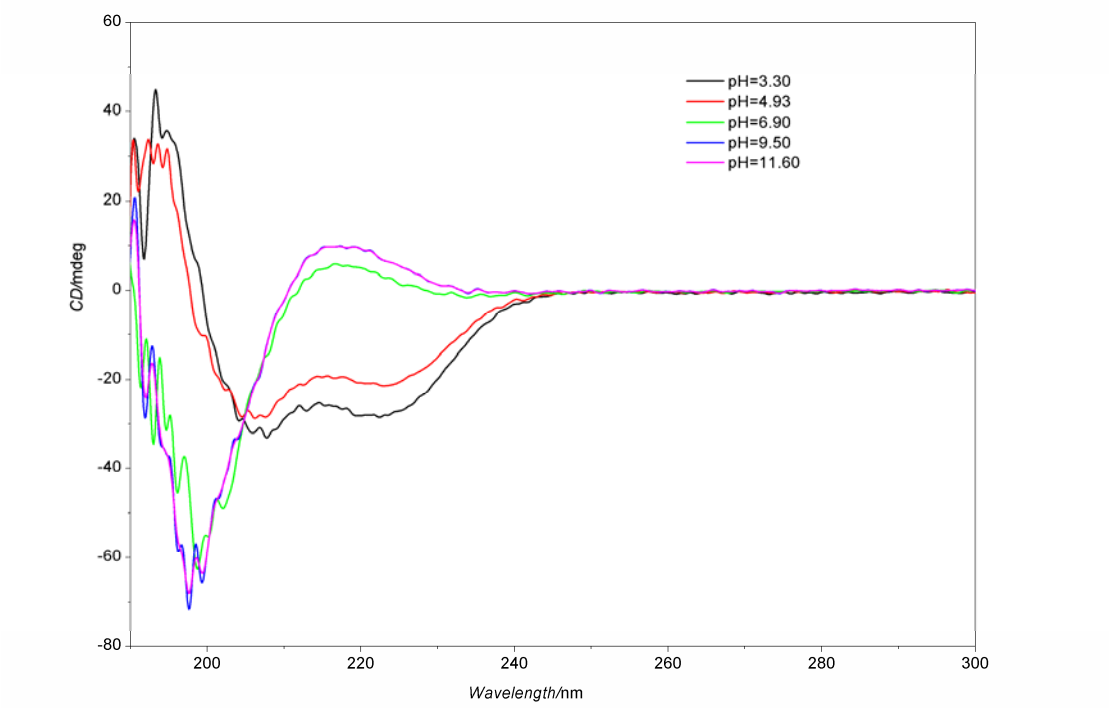

Fig. S8 CD spectra of $1FP_{170}$ in water at different pH values, 25 ℃, 0.2 mg mL^{-1}.

The pH-induced conformational change of polypeptide blocks was investigated by CD (Fig. S7). The CD spectrum of at $2FP_{33}$ above pH= 5.3 shows a typical curve with a small positive maximum at 218 nm, characteristic of a random coil conformation. When the pH value is decreased, the intensity of this positive maximum peak starts to decrease obviously at pH= 5.3. Therefore, we concluded that the coil-to-helix transition of $2FP_{33}$ block occurs between 5.3-4.28. Interestingly,

this result is not in agreement with the data reported in the literature,[S4] which indicated coil-to-helix transition happened around pH 7. When the pH value is decreased to 4.28, two negative minima at 222 and 208 nm could be detected, proving the formation of an α-helix conformation.[S5] It can be believed that this absolutely different conformational behaviors of $2FP_{33}$ results from its unique structure. It is helpful to compare the pH-induced conformational change of $2FP_{33}$ with that of poly(L-glutamic acid)-*b*-poly(propylene oxide)-*b*-poly(L-glutamic acid) (PLGA-*b*-PPO-*b*-PLGA) triblock copolymers, whose dependence of self-assembly behaviors in water on pH and temperature was investigated in detail by *J. P. Lin*.[S4b] The structures of $2FP_{33}$ and PLGA-*b*-PPO-*b*-PLGA were shown in Scheme S2.

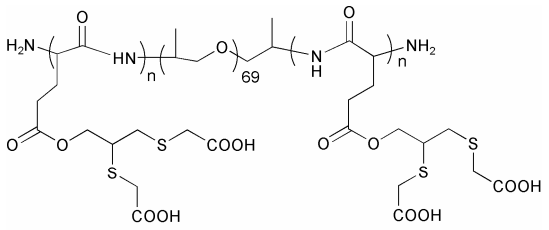

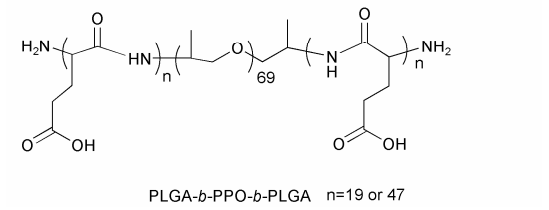

Scheme S2 Structure of $2FP_{33}$ and PLGA-*b*-PPO-*b*-PLGA.

In the work of *J. P. Lin*, the pH-induced conformational change of polypeptide blocks occurres around pH = 7, At higher pH values, the polypeptide blocks with coil form are extended due to the electrical repulsion between the PLGA residues. The repulsion decreases as pH value is decreased. At lower pH, the polypeptide blocks with helix form tend to shrink and have lower hydrophilicity. Here, α-helix conformation of $2FP_{33}$ even can be maintained between the pH value of 5.3 and 4.28, which is caused by the steric hindrance effect of the side chains of $2FP_{33}$. The characteristic of thiol-yne coupling is that two thiols can be coupled to one alkyne, adding the chemical complexity of polypeptide segments in copolymer of PPLG-*b*-PPO-*b*-PPLG. Finally, the obtained $2FP_{33}$ showed unique conformational behaviors in water under various pH values. The electrical effect competes with steric hindrance effect as pH value is decreased from 11 to 3.6 for $2FP_{33}$. For PLGA-*b*-PPO-*b*-PLGA ,when the pH value was lowered to 7, the electrical repulsion between the PLGA residues was reduced sharply, leading to the α-helix conformation at pH= 7 at once. Thus, he pH-induced conformational change of PLGA-*b*-PPO-*b*-PLGA was observed around pH = 7, However, for $2FP_{33}$ the steric hindrance effect inhibited the rapid transition of coil conformation to α-helix conformation when the pH value was lowered to 7, leading to the transition at much lower pH value (below 5.3).

Similarly, for $1FP_{170}$ the pH-induced conformational change of polypeptide blocks occurred in the pH region of 6.9 to 4.93 (Fig. S8). $1FP_{170}$ was used to control the biomineralization of $CaCO_3$ in water. CD spectra indicated that 1FP was effective in crystallization control when the polypeptide segments adopted a radom coil under alkaline conditions.

In summary, a preliminary study of secondary structure of the obtained polypeptide-based hybrid copolymers in bulk by FTIR shows that the polypeptide blocks adopt an α-helix

conformation. CD indicates that the functionalized polypeptide blocks in water exhabits a conformational change from random coil to α-helix as the pH value of the solution was decreased from 12 to 3.

8 Self-assembly behaviors of $2FP_{33}$ in water

In the main text, we observed that $2FP_{33}$ formed vesicles in water at pH value of 11.2. Here we carefully discussed the self-assembly of $2FP_{33}$ in water.

8.1 pH dependance of self-assembly behaviors of $2FP_{33}$ in water

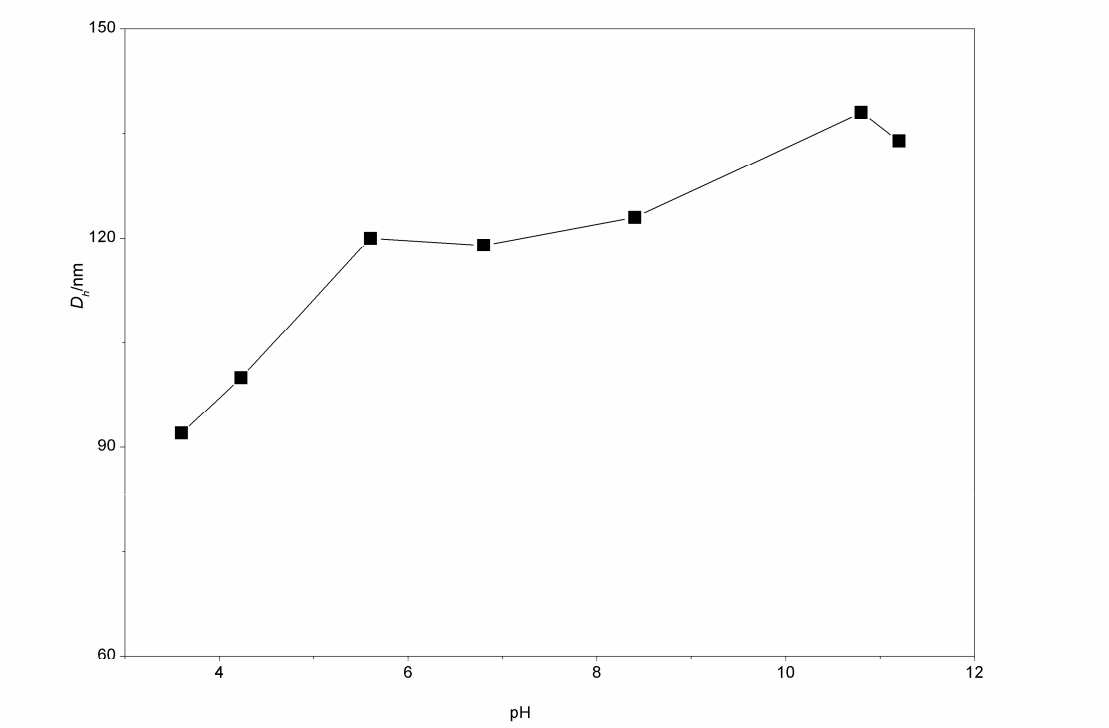

Fig. S9 The hydrodynamic diameter (D_h) of $2FP_{33}$ in water at various pH values, 25 ℃, 0.04 mg mL^{-1}, test angle of 90°.

The dependance of self-assembly behaviors of $2FP_{33}$ in water on pH value was monitored by DLS (Fig. S9). From Figure S9 it can be seen that the hydrodynamic diameter (D_h) is increasing when the pH value rises up. At pH=3.6 the D_h is 92 nm, and it is up to *ca.* 120 nm at pH 5.6. In fact, the D_h nearly keeps constant between the pH value of 5.6 and 8.4, and then it reaches to *ca.* 130 nm at pH value of 11.2. It should be noted that actually the D_h varies a little between the pH value of 5.6 and 11.2, less than 15 nm, which indicates that the micellae formed in water were stable in a broad pH region while the polypeptide blocks adopted a random coil conformation (as shown in Fig. S9). It is consistent with the observation of CD that the steric hindrance effect inhibited the rapid shrinking of micellae from a coil when the solution was adjusted to pH value below 7. Thus, it keeps the micellae stable until the pH was adjusted to 5.6.

8.2 Dependance of self-assembly behaviors of $2FP_{33}$ in water on temperature

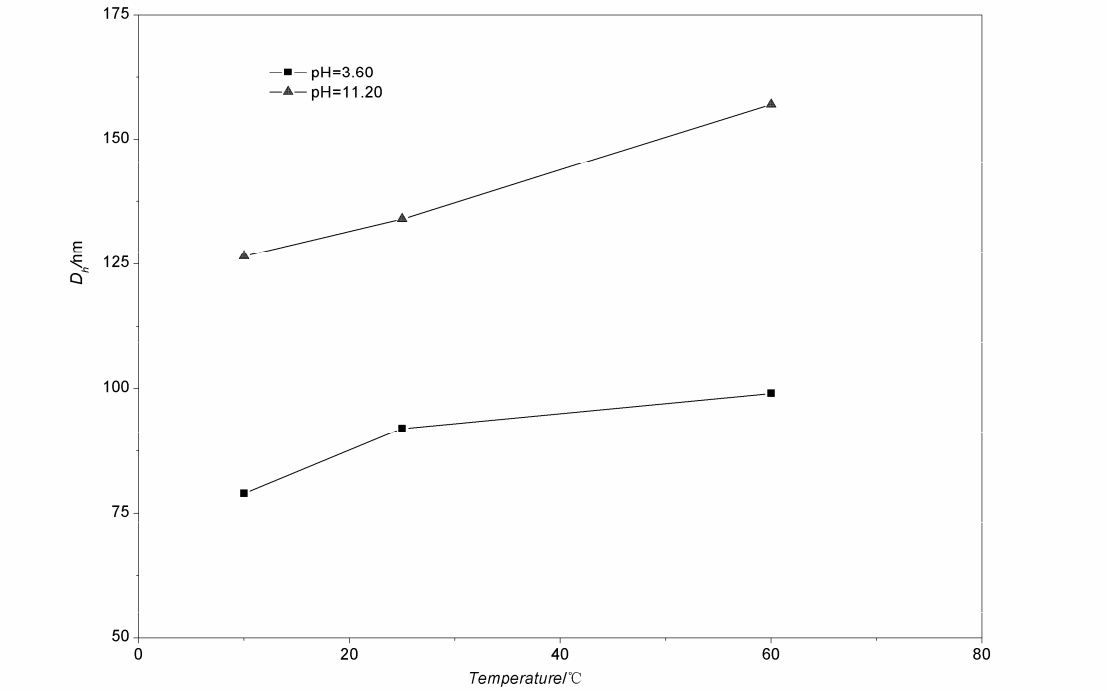

Fig. S10 The hydrodynamic diameter (D_h) of $2FP_{33}$ in water at various temperatures, 0.04 mg mL^{-1}, test angle of 90°.

Fig. S10 shows the D_h as a function of the temperature at pH=3.6 and 11.2. Note that all of the tests on D_h value were performed after the cell was equilibrated for about 1 h. The D_h of $2FP_{33}$ aggregates at pH=3.6 is 79 nm at 10 °C. With increasing temperature to 60 °C, the D_h increases to 99 nm. The D_h of $2FP_{33}$ aggregates at pH=11.2 is 127 nm at 10 °C. With temperature up to 60 °C, the D_h increases to 157 nm. In addition, the results revealed that the micellae at pH= 11.2 enlarged their size much more markedly than the micellae at pH= 3.6 with increasing temperature. Thus, the self-assembly behaviors of 2FP33 is pH- and thermosensitive, which results from the thermoresponse property of PPO blocks.[S6]

8.3 Morphology observation of the self-assemblies by TEM and AFM

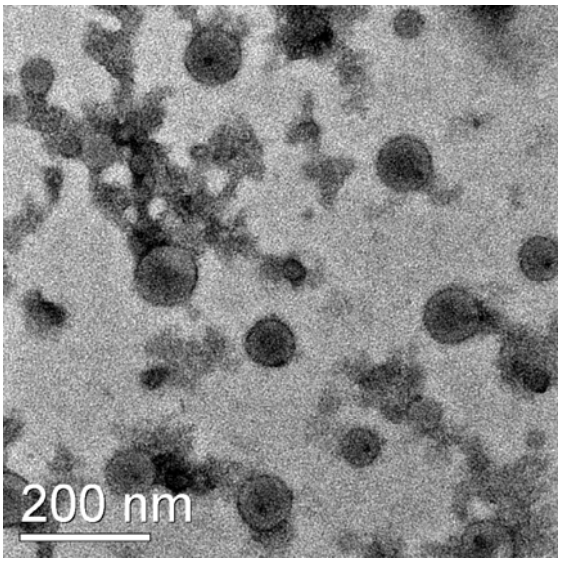

Fig. S11 The TEM image of micellae formed by 2FP33 in water at pH =3.6, 0.04 mg mL^{-1}, 25 °C.

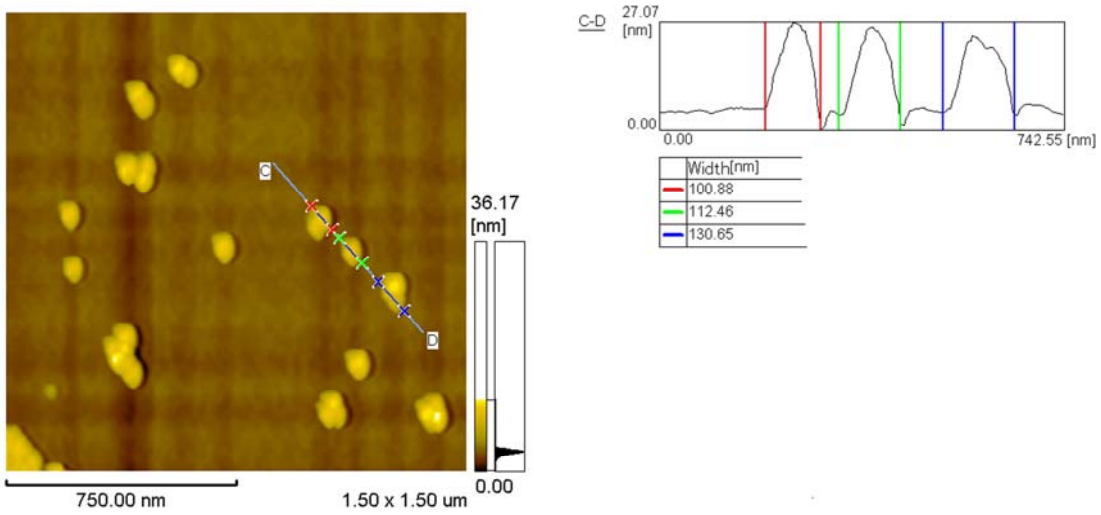

Fig. S12 The AFM image of micellae formed by 2FP33 in water with concentration of 0.04 mg mL^{-1} at pH =3.6, 25 °C

As described above and in the main text, the aggregates formed by $2FP_{33}$ at pH=11.2 are vesicles, which was proved by SLS and TEM. Here, morphology of the self-assemblies of $2FP_{33}$ in water at pH=3.6 was investigated by TEM and AFM. The TEM image of $2FP_{33}$ indicates that the aggregates seemingly has a spherical morphology in the size of *ca.* 90 nm consistent with the DLS results (Fig. S11), however, AFM revealed that the aggregates are lamellar in the height of *ca.* 25 nm and width of *ca.* 100-130 nm.

In summary, $2FP_{33}$ forms vesicles under alkaline conditions, and the vesicles change their morphology into lamella under acidic conditions. The micellae formed by $2FP_{33}$ in water is pH- and thermosensitive, showing a pH and temperature double-response behavior.

8.4 Determination of R_g of $2FP_{33}$ aggregates in water by SLS

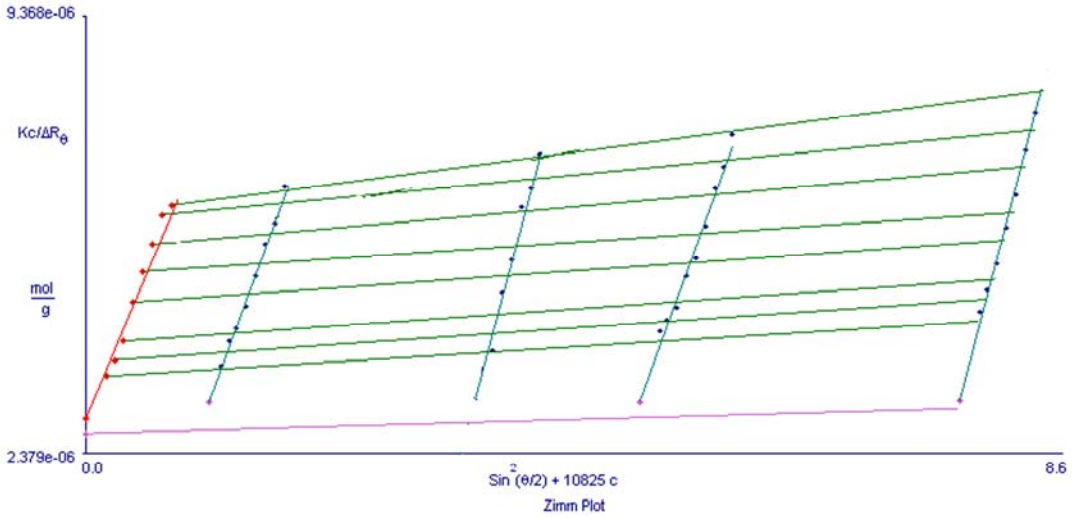

Fig S13 Zimm Plot of $2FP_{33}$ in water at pH = 11.20, 25 °C.

A radius of gyration 63 nm was obtained by the Zimm plot analysis. The DLS analysis performed at 90° angle for $2FP_{33}$ under pH = 11.2 provided a hydrodynamic radius (R_h) of 67 nm (as shown in Fig. S9). Thus, the ratio $\rho=R_g/R_h$ used as the indicator of morphology is 0.94, close to the theoretical value of 1.0 for a vesicle morphology.

9 The biomineralization process of $CaCO_3$ in water directed by 1FP

1FP can be used to control the biomineralization of $CaCO_3$. Polypeptide-based double hydrophilic (DHBCs) hybrid copolymers have been used to direct the biomineralization process of $CaCO_3$ in water or water/organic solvents mixed solutions.[S7]

The polepeptide blocks of 1FP, which have a high affinity for Ca^{2+} ions as a result of the presence of -COOH, provide sites for Ca^{2+} concentration. This mechanism induces the local supersaturation of Ca^{2+} that is necessary for mineral nucleation. At the same time, the hydrophilic polypeptide segments aid in keeping the growing crystal nucleus in solution, resulting in a spherical morphology at pH =10. Of course, this process can be affected by pH, temperature and length of polypeptide blocks and so on, leading to the diverse morphology of $CaCO_3$ (as shown in the main text). Although results of CD showed that 1FP was effective in crystallization control when the polypeptide segments adopted a radom coil under alkaline conditions, it does not mean that the conformation of polypeptide has no effect on the morphology of $CaCO_3$. This process was investigated under alkaline conditions just because $CaCO_3$ can not be formed in acidic conditions. It also can be believed 1FP can be used to control the crystallization of other minerals except $CaCO_3$.

References

[S1] (a) W. H. Daly and D. Poche, *Tetrahedron Lett*, 1988, **29**, 5859; (b) D. S. Poche, M. J. Moore and J. W. Bowles, *Synth. Commun*, 1999, **29**, 843.

[S2] Y. Masuda and T. Miyazawa, *Makromol. Chem*, 1967, **103**, 261.

[S3] H. A. Klok, J. F. Langenwalter and S. Lecommandoux, *Macromolecules*, 2000, **33**, 7819; (b) P. Papadopoulos, G. Floudas, H. A. Klok, I. Schnell and T. Pakula, *Biomacromolecules*, 2004, **5**, 81.

[S4] (a) F. Checot, A. Brulet, J. Oberdisse, Y. Gnanou, O. Mondain-Monval and S. Lecommandoux, *Langmuir*, 2005, **21**, 4308; (b) C. H. Cai, L. S. Zhang, J. P. Lin and L. Q. wang, *J. Phys. Chem. B*, 2008, **112**, 12666.

[S5] G. Holtzwarth and P. Doty, *J. Am. Chem. Soc*, 1965, **87**, 218.

[S6] (a) T. Nivaggioli, B. Tsao, P. Alexandridis and T. A. Hatton, *Langmuir,*1995, **11**, 119; (b) N. J. Jain, V. K. Aswal, P. S. Goyal and P. Bahadur, *J. Phys. Chem. B*, 1998, **102**, 8452.

[S7] (a) S, H. Yu and H. Cölfen, *J. Mater. Chem*, 2004, **14,** 2124; (b) L. E. Euliss, T. M. Trnka, T. J. Deming and G. D. Stucky, *Chem. Commun*, 2004, **4**, 1736; (c) H. A. Klok, *Macromolecules,* 2009, **42**, 7990.